



Influence of Nickel Modified Beta Zeolite in the Production of BTEX During Analytical Pyrolysis of Medium-Density Fiberboard (MDF)

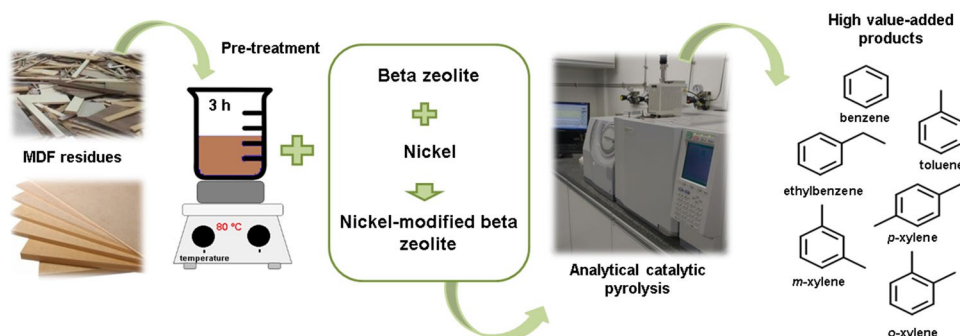
Francieli Martins Mayer^{1,2} · Ana Paula Stelzer de Oliveira¹ · Daliomar Lourenço de Oliveira Junior³ · Bruna Carla Agustini⁴ · Gildo Almeida da Silva⁴ · Eduardo Hiromitsu Tanabe³ · Doris Ruiz⁵ · Maria do Carmo Rangel^{1,2} · Claudia Alcaraz Zini¹

Received: 13 March 2021 / Accepted: 30 September 2021
© The Author(s), under exclusive licence to Springer Nature B.V. 2021

Abstract

Production of high added value chemicals such as BTEX by means of catalytic fast pyrolysis of MDF residues is a promising and environmentally friendly alternative to fossil fuels, as MDF is abundantly produced worldwide. Generation of toxic compounds during MDF pyrolyses was minimized with pre-treatments with yeasts or hot water resulting in a maximum removal of 87.9% of nitrogen compounds when water was used at 80 °C, for 3 h. Nickel-modified beta zeolites with 3 (Ni3B-H) and 5 wt% of nickel (Ni5B-H) were more efficient for the production of BTEX compounds (Ni3B-H: 39.35% and Ni5B-H: 38.65%) and reduction of polyaromatic hydrocarbons (Ni3B-H: 11.12% and Ni5B-H: 15.93%) when compared to pure beta zeolite. Non-catalytic pyrolysis resulted only in oxygenated compounds. These findings were related to the changes of the crystallographic sites of aluminum and then on acidic sites, as well as to the production of a bifunctional catalyst during reactions.

Graphic Abstract



Keywords BTEX · Medium-density fiberboard · Catalytic pyrolysis · Nickel-modified beta zeolite · Gas chromatography/mass spectrometry

Statement of Novelty

A simple water washing step of MDF toxic wastes followed by pyrolysis with Ni-modified beta zeolite allows the production of BTEX, as an innovative answer to a

major environmental problem. This is the first process for BTEX production in one step over Ni-modified beta zeolite from MDF pyrolysis.

✉ Maria do Carmo Rangel
maria.rangel@ufrgs.br

✉ Claudia Alcaraz Zini

Extended author information available on the last page of the article

Introduction

The medium-density fiberboard (MDF) residues are highly available lignocellulosic biomasses for power generation, because of the great volume of MDF produced and of the increasing demand from the furniture industry worldwide. According to the annual report of the IBÁ (*Indústria Brasileira de Árvores*), the eight biggest producers wood panels are together responsible for 176.7 million m³ of them in 2019. The Brazilian production (eighth-largest producer in the world) corresponded to 8.2 million m³ [1]. In general, MDF residues contain nitrogen due to the addition of synthetic resins [urea–formaldehyde (UF), phenol–formaldehyde (PF) and melamine–formaldehyde (MF)] during production and/or finishing stages of MDF production. These nitrogen-containing compounds (N-compounds) are responsible for the formation of toxic compounds (hydrocyanic acid, isocyanic acid, and ammonia) during thermal processing (combustion and pyrolysis) of the residue, as well as for the constant release of formaldehyde from panels [2]. Therefore, a pre-treatment of MDF residues to remove the N-compounds is an alternative to make a safer subsequent pyrolysis step and also to minimize the toxicity of these residues.

Biological pre-treatments have the advantages of being non-toxic, consuming less energy and generating no waste, therefore being environmentally friendly. The use of fungal and bacterial strains or their enzymes to delignify microalgae and lignocellulosic biomass has achieved promising results when the objective was the increase of biomass conversion to biofuels in a following step [3, 4]. The removal of N-compounds from other matrices, such as domestic, industrial and agricultural wastewaters, to prevent eutrophication and pollution of aquatic environments is commonly performed through well-defined processes (nitrification and denitrification) [5]. However, these procedures are carried out in two stages, are time consuming, and present limitations when the effluent has high loads of nitrogen. For these reasons, researchers have looked for alternative biological treatment, such as the use of duckweeds, which has shown advantages over conventional methods [6]. Extractability tests of MDF resins (UF, PF, and MF) have shown that they are susceptible to hydrolysis [7]. Therefore, a pre-treatment involving a water washing step seems to be also a viable and simple possibility to remove MDF N-compounds. Besides nitrogen removal, this kind of washing pretreatment can be useful to remove ash from biomass, and improve the yield of bio-oil [8, 9].

The fast pyrolysis of MDF residues have been proven useful for producing fuels and/or high added value compounds, but the bio-oil obtained has limited applications because of the high amounts of phenolic and other oxygen-containing

compounds (O-compounds) [2, 10]. It is known [11, 12] that the use of catalysts can overcome this drawback, favoring the production of more valuable compounds for the industry as well as tailoring products distribution. Various catalysts have been used in pyrolysis, being zeolites the most attractive ones to produce aromatic hydrocarbons (AH) [11]. Among zeolites, ZSM-5 has been extensively studied [10, 12–15] because of its high acidity. However, its application is limited to model molecules such as phenol and other monoaromatics. Since the first works, it has been noted that the large molecules of biomass could not go into the small pores of ZSM-5 to access the catalytic active sites. This hindered its application to larger molecules or to biomasses, due to several consequences such as coke formation in the pores, fast catalyst deactivation and then low conversion rates. Therefore, various alternatives have been emerged, such as the addition of metals to HZSM-5 and the use of other zeolites.

In attempt to improve the catalytic performance of HZSM-5, by reducing coke formation and increasing the production of aromatics, in a previous study of our group (2018), HZSM-5 pure and modified with cobalt, iron, nickel, niobium and zinc were evaluated in pyrolysis of MDF residues. Among the catalysts, nickel-modified HZSM-5 has shown the best performance, increasing the selectivity to BTEX and the reduction of polyaromatic hydrocarbons (PAH) and O-compounds amounts in pyrolytic vapors of MDF residues [10]. These results have motivated our group to investigate the catalytic properties of nickel supported on a large pore zeolite, such as beta zeolite ($\sim 6 \times \sim 7$ Å). Larger pores facilitate the diffusion of primary thermal degradation compounds of biomass components, improving the conversion and the catalyst stability even more.

However, beta zeolite can also provide enough space for the formation of large compounds such as PAH, which are coke precursors, responsible for catalyst deactivation [16–18]. Moreover, PAH are not desirable in bio-oil due to their high toxicity and carcinogenicity [19]. However, this drawback is expected to be overcome by metals in zeolite channels, which allow to tailor the zeolite properties and then improve the products distribution and bio-oil yield, besides decreasing coke formation [11]. Among various transition metals used as catalysts, nickel stands out for promoting reactions of oligomerization, dehydration, hydrogenation/dehydrogenation and ring-opening, among others. In addition, it increases the hydrothermal stability of the catalyst and have an appropriate cost–benefit ratio [17]. Moreover, nickel-modified beta zeolite has been used in heavy oil upgrading to produce BTEX. The acidic and metallic sites favoured the ring-opening reactions in double or more ring molecules through two stages (hydrogenation and cracking) [20, 21]. Beta zeolite-supported nickel was also used as a

catalyst in the hydroreforming of an oil resulting from the thermal cracking of polyethylene to produce fuel [22].

By considering the properties of nickel and beta zeolite, catalysts with different amounts of nickel supported on beta zeolite were studied in this work, as a new alternative to fast pyrolysis of biomass. As far as we know, these catalysts have not been evaluated in biomass pyrolysis yet. In addition, there is no report of pyrolysis of MDF performed over catalysts based on beta zeolite-supported nickel. Also, it is the first time that removal of nitrogen content is proposed through washing with water and biological treatment of lignocellulosic biomass.

The production of MAH, especially BTEX from renewable sources, arouses great interest in academia and industry, considering that their current production occurs exclusively through petroleum cracking. The BTEX compounds are used in several branches of industry, being the raw material in the manufacture of a large variety of products (solvents, plastics, detergents, cosmetics, pharmaceuticals, among others) [17, 23, 24]. For this reason, the production of BTEX through alternative sources such as catalytic pyrolysis of residual biomass, is a promising proposal.

The preparation, characterization, and evaluation of beta zeolite-supported nickel are described to demonstrate the potential of this system as alternative catalyst for producing BTEX during catalytic pyrolysis of MDF. An efficient, low cost and simple pre-treatment method for the removal of N-compounds from residual MDF biomass containing melamine coating is also proposed, as a solution to solve MDF toxicity.

Materials and Methods

Raw Material and Pre-treatment

MDF residues from eucalyptus wood covered with melamine laminated paper were employed as raw material and were provided by the Institute of Technology in Wood and Furniture (CETEMO, *Centro Tecnológico do Mobiliário*) of National Service of Industrial Training (SENAI, *Serviço Nacional de Aprendizagem Industrial*). The reasons for choosing this specific biomass and its composition have been published in a former study of our group [10].

The removal of N-compounds from MDF residues was studied through two different pre-treatments: biological and washing with distilled water. The biological pre-treatment was developed with thirty two yeasts from the Collection of Micro-organisms of Agro-industrial Interest (CMIA, *Coleção de Microrganismos de Interesse Agroindustrial*) of EMBRAPA. Information about the collections of micro-organisms can be found in the Online Resource 1 (Table

ESM1). Firstly, the screening of the yeasts was carried out through a nitrogen assimilation test (auxanogram) in a solid medium. Petri dishes were incubated at 25 °C and their visual examination was performed every 24 h. Yeasts that grew with residues as the sole source of nitrogen were subjected to another nitrogen assimilation test in liquid medium, and again with residual MDF being the only source of nitrogen. The nitrogen assimilation profile of the yeasts was performed both in liquid and on solid media, with Yeast Carbon Base (Difco, Franklin Lakes, USA), as previously described [25, 26]. After preliminary tests with the 32 yeasts, one yeast (100 µL of a suspension of cells containing 10^7 cells mL⁻¹) was chosen to be further evaluated through eight (8) days of incubation in a liquid medium at 25 °C in a Psycrotherm (150 rpm, New Brunswick, USA) rotary shaker. In a following step, the content was centrifuged, and the precipitate was washed with deionized water at 23 °C for the total removal of the yeast cells. The resulting samples were dried at room temperature and named MDF-Y. A control sample of MDF (MDF-Y0) was incubated with water in the same conditions without the addition of yeasts to the process. Biological pre-treatment tests were all performed in triplicate.

The washing with distilled water was conducted at three different temperatures [7]. Firstly, three (3) g of MDF were placed inside a beaker containing two hundred (200) mL of distilled water. The water/biomass mixture was stirred (model RH basic 2, IKA, São Paulo, Brazil) for twenty-four (24) h at ~3 °C and designated as MDF23. The same type of mixture underwent stirring for three (3) h at 80 °C, in a second beaker (MDF80). A third beaker with similar mixture was heated at 100 °C for 2 h (MDF100). Whenever necessary, more pre-heated distilled water was added to the mixture during biomass heating to adjust the initial volume. The pre-treated MDF samples were filtered with qualitative paper filter and dried at ~23 °C. Elemental analyses of all MDF samples that were biologically pre-treated or washed with distilled water have been carried out, as well as with non treated samples in order to evaluate the removal of N-compounds. Analysis of variance was performed with data obtained and the means were compared by Tukey's test ($p \leq 0.05$). Before pyrolysis, pre-treated and non pre-treated MDF samples were dried in an oven at 40 °C (~12 h) to constant weight (Model 315 SE, FANEM, São Paulo, Brazil). Biomass particles size ranged from 0.25 to 0.43 mm (40–60 mesh; Bertel, São Paulo, Brazil), according to a previous study [10].

Nickel-Modified Beta Zeolite Synthesis

The synthesis of beta zeolite followed a modified Vaudry's methodology [27] using commercial silica Aerosil 200 (Degussa, Frankfurt, Germany). The catalyst acid form

(B-H) was obtained through ion exchange. B-H loaded with nickel has been prepared by a wet impregnation method with an aqueous solution of nickel nitrate (Synth, São Paulo, Brazil) to obtain concentrations of 3 and 5 w/w % of nickel in the final solid. These samples were dried at 110 °C, for 24 h and the solids obtained were calcined at 550 °C (2 °C min⁻¹) for 5 h. The catalysts were denominated Ni3B-H and Ni5B-H according to nickel concentration in the solid, as 3 and 5 w/w% of nickel, respectively.

Nickel-Modified Beta Zeolite Characterization

Powder X-ray diffraction (XRD) patterns were recorded on an Ultima IV diffractometer (Rigaku, Honshu, Japan), using Cu-K α radiation in the 2 θ range of 5° to 50°. The relative crystallinity of the catalysts was calculated according Bhat and Kumar [28]. When nickel oxide crystals could be identified their average diameter has been determined by the Scherrer equation [29].

The silica to alumina ratio (SAR), as well as nickel loadings on the beta zeolite catalysts were determined by Flame Atomic Absorption Spectrometry (FAAS) using a Perkin Elmer A Analyst 200 apparatus (PerkinElmer, Massachusetts, USA) equipped with hollow cathode lamp (LUMI-NATM, PerkinElmer).

Nitrogen adsorption measurements were obtained in a Micromeritics (Model TriStart II 3020, Georgia, USA) apparatus. Before adsorption, beta zeolite catalysts were conditioned under vacuum at 150 °C for 12 h to remove water and gases from the pores of the samples. Brunauer–Emmett–Teller (BET) specific areas were determined using the BET theory. The microporous volumes (V_{micro}) were calculated via t -plot method using Harkins and Jura equation. Mesoporous volume (V_{meso}) and pore diameter (d_p) were determined following Barret–Joyner–Halenda (BJH) method.

²⁹Si and ²⁷Al NMR spectra of the samples were recorded at 500 MHz and 11.7 T in a model dd2 narrow bore model Agilent Technologies spectrometer. All measurements were carried out at room temperature. For obtaining the ²⁹Si spectra, the following conditions were used: contact time: 7 ms, relaxation time: 5 s, pw90H1: 2.9 μ s, pq90C13: 2.55 μ s and rotor spinning: 10 kHz. The ²⁷Al spectra were obtained under the following conditions: relaxation time: 10 s, pw90A127: 14 μ s and rotor spinning: 10 kHz.

Acidic characteristics of the catalysts (B-H, Ni3B-H and Ni5B-H) have been measured by ammonia temperature-programmed desorption (NH₃-TPD, Micromeritics AutoChem II) equipped with a thermal conductivity detector (TCD). In addition, the type of acid sites (Brønsted or Lewis acid site) was determined through pyridine adsorption followed by Infra Red (IR) spectroscopy (Shimadzu Prestige 2, Kyoto, Japan).

Catalytic and Non-catalytic Analytical Pyrolysis

EGA/Py-3030D (Frontier Laboratories Ltd, Fukushima, Japan) connected to a GC/qMS (QP2010-Ultra Shimadzu) was used in catalytic and non-catalytic analytical pyrolyses. For each experiment, 500 μ g of biomass was placed inside the stainless-steel ecological cup (eco-cup, 4 mm outside diameter \times 5 mm height, 50 μ L). A mass of 2.5 mg of catalyst (ratio of 5 catalyst/biomass) was added on top of the biomass in the eco-cup, whenever catalytic pyrolysis was carried out. Biomass and catalysts were weighted in an analytical balance (Model AUW220D, Shimadzu) [10, 16]. Pyrolyses were performed at 500 °C for 15 s. The eco-cup containing the sample was released into the oven whenever its temperature reached 500 \pm 0.1 °C. During pyrolyses, helium gas flow (purity of 99.999%, White Martins, Rio Grande do Sul, Brazil) was used to purge the system and to provide inert atmosphere (100 mL min⁻¹). The condensable vapors were carried to an injector at 280 °C and operated in split mode (split ratio 1/30). GC/qMS instrument was equipped with a DB-5MS capillary column (30 m \times 0.25 mm \times 0.25 μ m 5%, Agilent Technologies, Santa Clara, USA). All pyrolytic processes have been performed in duplicate. The compounds were tentatively identified using retention indices and mass spectral data and a semi quantitative approach has been employed to reach chromatographic area percentage of each peak. Both methodologies and other chromatographic conditions are reported in a former study of our group [10].

Results and Discussion

Biomass Pre-treatment

The results of elemental analyses of MDF residual biomass and pre-treated MDF are presented in Table 1, where the content of nitrogen allows us to infer which pre-treatments are the most efficient for nitrogen removal. A preliminary screening has been performed with 32 yeast strains, where MDF was the only source of nitrogen. Among the 32 incubated yeasts, only the *Pichia kluyveri* BRM 028949 and *Saccharomyces cerevisiae* BRM 004687 showed some growth zone using MDF as the sole source of nitrogen. *Pichia kluyveri* BRM 028949 (sample MDF-Y in Table 1) gave the best results during the preliminary scanning and was chosen to be employed in a biological pre-treatment of residual MDF. Comparing the reduction of nitrogen content caused by *P. kluyveri* pre-treatment (66.7%) with the control sample (12.1% in MDF-Y0), the yeast has shown to be a significant aid in this process. The percentage of nitrogen reduction in the blank may be explained by the partial solubility of MDF resins in water. Even though these results are preliminary and further studies are necessary to

Table 1 Average values and standard deviations of elemental analyses results for residual MDF samples and of samples that underwent pre-treatment with yeasts and with distilled water at different temperatures

| Pre-treatment | Carbon % \pm SD | Hydrogen | Nitrogen | Reduction of nitrogen (%) |
|---------------|--------------------------------|------------------------------|-------------------------------|---------------------------|
| MDF | 44.0 ¹ \pm 0.8 a | 5.9 ¹ \pm 0.2 a | 3.3 ¹ \pm 0.2 a | – |
| MDF-Y0 | 44.5 ² \pm 0.1 ab | 6.0 ² \pm 0.1 a | 2.9 ² \pm 0.0 ac | 12.1 |
| MDF-Y | 44.8 ² \pm 0.0 ab | 6.1 ² \pm 0.1 a | 1.1 ² \pm 0.1 d | 66.7 |
| MDF23 | 44.6 ¹ \pm 0.3 ab | 6.0 ¹ \pm 0.1 a | 2.5 ¹ \pm 0.4 c | 24.2 |
| MDF80 | 45.2 ¹ \pm 0.4 b | 6.0 ¹ \pm 0.1 a | 0.4 ¹ \pm 0.1 b | 87.9 |
| MDF100 | 45.2 ¹ \pm 0.3 b | 5.9 ¹ \pm 0.3 a | 0.2 ¹ \pm 0.0 b | 93.9 |

SD standard deviation, MDF residual MDF from eucalyptus wood covered with melamine laminated paper, MDF-Y0 control sample during the biological pre-treatment, MDF-Y MDF sample that underwent pre-treatment with *Pichia kluyveri* BRM 028949; MDF23, MDF80, and MDF100: MDF samples that were washed with distilled water at 23 °C, 80 °C and at boiling point, respectively. Average values in the same column followed by the same letter do not present significant difference, according to Tukey's test ($p \leq 0.05$). Experimental description is reported in Sect. Raw Material and Pre-treatment

¹Average results of a triplicate pre-treatment process and of duplicate elemental analyses

²Average results of duplicate elemental analyses

optimize the experimental conditions (temperature and time of incubation), the data obtained are encouraging. Examples of the application of yeasts to lignocellulosic biomass have been restricted to lignin removal and in these cases, the time of incubation is higher than one week and may take a few months [4]. There is no report about employing yeasts as a pre-treatment of lignocellulosic biomass for the removal of N-compounds, although biological treatment has been employed for a long while to domestic, industrial and agricultural wastewater treatment with a removal > 90% [5].

Table 1 also shows the nitrogen percentage of samples that underwent washing with distilled water at different temperatures. Water washing at 80 °C (MDF80) and boiling water (MDF100) produced the best results as biomass pre-treatment: 87.9 and 93.9% of nitrogen reduction, respectively. It means that the risk of producing toxic compounds during pyrolysis of biomass has been substantially reduced with this simple and non-expensive biomass pre-treatment. Conversely, washing MDF with distilled water at room temperature (~ 23 °C) resulted only in 24.2% of nitrogen reduction. The temperature of 80 °C allows a simpler experimental control (no replacement of water) and less energy consumption in comparison to boiling water, not only in laboratory experiments but also in future pilot and industrial plants.

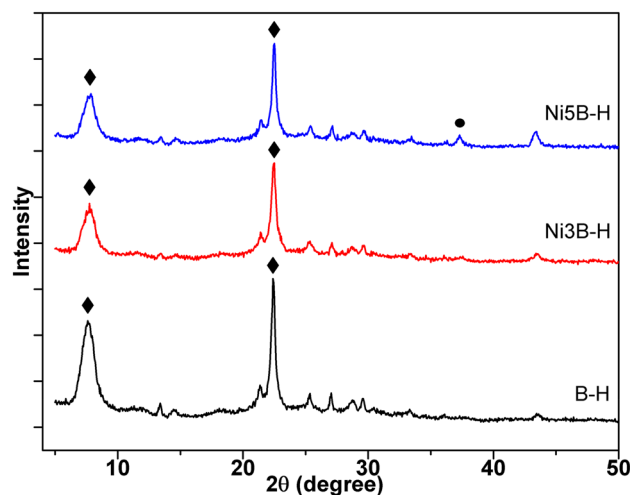


Fig. 1 XRD diffractograms for Ni3B-H, Ni5B-H (3 and 5% nickel modified beta zeolite), and pure beta zeolite (B-H). Diffraction peaks correspond to (filled diamond) beta zeolite and (filled circle) nickel oxide. Experimental procedures are described in Sects. Nickel-Modified Beta Zeolite Synthesis and Characterization

Nitrogen content of MDF pre-treated with hot water (80 and 100 °C) has shown to be similar to a great variety of lignocellulosic biomasses, according to a recent published review about the chemical characterization (CHN) of this type of matrices (0.01–0.6%) [30]. For all these reasons, MDF residues have been pre-treated with distilled water at 80 °C before pyrolysis. On the other hand, pre-treatment with *Pichia kluyveri* BRM 028949 (MDF-Y) has also reached low levels of nitrogen content presenting great potential as a promising alternative, after optimization of experimental conditions. Biological processes are considered environmentally friendly as yeasts are not toxic and do not generate residues, requiring low energy input. However, it is likely that long periods of incubation may be needed to reach satisfactory results [3, 4].

Catalysts Characterization

XRD patterns of all catalysts (B-H, Ni3B-H, and Ni5B-H) are exhibited in Fig. 1. All diffractograms presented the pattern of beta zeolite ($2\theta = 7.8^\circ$ and 22.4°) indicating that the zeolite framework was preserved after impregnation thermal treatment, in accordance with previous work [31]. The decrease of the intensity of the peaks related to beta zeolite ($2\theta = 7.8^\circ$ and 22.4°) observed for nickel catalysts indicated a decrease of crystalline domains after impregnation with nickel. The peak attributed to NiO species were detected in $2\theta \sim 37.3^\circ$ only in the XRD patterns of Ni5B-H. The average crystal (NiO) size was estimated as 18.8 nm by the Scherrer equation (based in the 37.3° reflection). No additional peak was detected in the Ni3B-H XRD pattern, probably due to

the small size of nickel oxide crystals and/or due to its low concentration.

The experimental values of nickel content (determination by FAAS), were close to the expected ones, as shown in Table 2. Beta zeolite showed a SAR value of 18, which is also according to the expected value. The textural properties for beta zeolite catalysts are also shown in the Table 2. The BET specific area of B-H ($547 \text{ m}^2 \text{ g}^{-1}$) is in accordance with previously reported data for beta zeolite ($559\text{--}618 \text{ m}^2 \text{ g}^{-1}$) [17, 20, 22, 31]. After impregnation, data corresponding to BET specific area and also to microporous volume changed within the experimental error (10%). This indicates that the NiO crystals detected in the diffractogram did not block the pores of the Ni5B-H, most likely because the crystals (NiO = 18.8 nm) were bigger than the pores of the catalyst (7–11 nm, Table 2). This behavior has been already observed for beta zeolites in a study of Escola et al. However, it is well-known that it depends on the nature and loading of the metal, as well as on the type of zeolite [31, 32]. Nickel catalysts showed decreased mesoporous volume, if compared to B-H (Table 2). This suggests that nickel particles are probably located inside these interparticles mesopores.

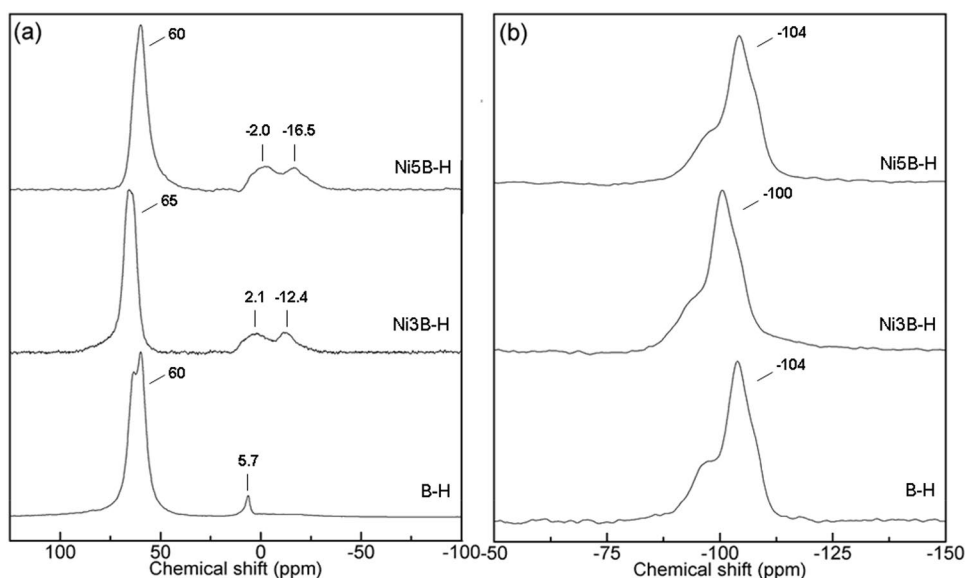
The solid-state ^{27}Al NMR spectra of the catalysts (Fig. 2a) were obtained to better understand the relationship between the intrinsic acidity and catalytic activity of zeolites, both closely related to the chemical environment of aluminum. The framework of aluminum atoms in tetrahedral coordination (Al_{Td}) in beta zeolite, for instance, can be easily distinguished from extra-framework aluminum atoms in octahedral position (Al_{Oh}) due to different chemical shifts at 50–80 ppm and around 0 ppm, respectively [33]. The ^{27}Al NMR spectra of B-H shows signals centered at 60 and 5.7 ppm (Fig. 2a). The first peak is broad indicating that aluminum atoms are occupying different tetrahedral positions in the disordered structure of B-H. As pointed out earlier [34], the crystalline structure of beta zeolite comes from the intergrowth of two or three polymorphs (A, B, C), generating high concentration of stacking defects coming from the partially coordinated aluminum. Depending on the polymorphs in the zeolite, the spectrum may contain up to nine crystallographic tetrahedral (T) sites [35, 36], which can be identified by MQ MAS NMR technique (Multiple-Quantum Magic-Angle Spinning NMR). Comparing these works with ours, the peak at 60 ppm can be associated to T3 or T4 crystallographic sites ($\text{Al}(\text{IV})_{\text{a}}$), the width of the lines being related to a distribution in isotropic chemical shifts, determined by changes in Al–O–Si angles [33, 37]. These contributions come from the normal framework (non distorted tetrahedral aluminum) and from a distorted tetrahedral aluminum [37]. According to previous works [35], the position and distribution of aluminum in zeolite framework depend on the conditions of zeolite preparation as well as on the Si/Al ratio. A similar profile was displayed by the Ni5B-H sample, indicating that these crystallographic

Table 2 Chemical composition, textural properties and distribution of acid sites for pure beta zeolite (B-H) and beta zeolite impregnated with 3 and 5% of nickel (Ni3B-H and Ni5B-H, respectively)

| Catalyst | $\text{Al}_{\text{Td}}/\text{Al}_{\text{Oh}}$ | Ni (wt%) | $A_{\text{BET}}^{\text{a}}$ ($\text{m}^2 \text{ g}^{-1}$) | $V_{\text{micro}}^{\text{a}}$ ($\text{cm}^3 \text{ g}^{-1}$) | $V_{\text{meso}}^{\text{a}}$ ($\text{cm}^3 \text{ g}^{-1}$) | d_{p}^{a} (nm) | T_{max} ($^{\circ}\text{C}$) | Distribution of acid sites ($\mu\text{mol g}^{-1}$) | | | Total amount acid sites ($\mu\text{mol g}^{-1}$) | | |
|----------|---|----------|---|--|---|--------------------------------|---|---|-----|--------|--|-------|--------|
| | | | | | | | | T1 | T2 | T3 | | Weak | Strong |
| B-H | 4.2 | – | 547 | 0.15 | 0.31 | 11 | 145 | 343 | – | 605.9 | 254.8 | – | 860.7 |
| Ni3B-H | 8.4 | 3.4 | 525 | 0.17 | 0.17 | 7.4 | 163 | 341 | 504 | 1231.8 | 344.3 | 336.6 | 1912.7 |
| Ni5B-H | 7.1 | 5.5 | 497 | 0.16 | 0.13 | 11 | 156 | 337 | 484 | 1091.5 | 413.1 | 490.9 | 1995.5 |

^aThe estimated measurement error is < 10%; $\text{Al}_{\text{Td}}/\text{Al}_{\text{Oh}}$: aluminum in tetrahedral position to aluminum in octahedral position ratio; A_{BET} : BET specific area; V_{micro} : micropore volume calculated using *t*-plot method; V_{meso} : mesopore volume calculated using BJH method; d_{p} : pore diameter (nm) calculated using BJH method; T1: maximum desorption temperature of weak acid sites; T2: maximum desorption temperature of strong acid sites; T3: maximum desorption temperature of stronger acid sites. Acid characteristics were determined by NH_3 -TPD. Experimental procedures are described in Sects. Nickel-Modified Beta Zeolite Synthesis and Characterization

Fig. 2 **a** ^{27}Al NMR and **b** ^{29}Si NMR spectra of B-H (pure beta zeolite), Ni3B-H and Ni5B-H (3 and 5% nickel modified beta zeolite). Experimental procedures are described in Sects. Nickel-Modified Beta Zeolite Synthesis and Characterization



sites were not significantly affected by nickel. However, the Ni3B-H spectrum showed a peak shifted to higher values, indicating that aluminum atoms were moved to different crystallographic sites and had experienced different chemical environments.

The other peak at 5.7 ppm in B-H would be expected to occur at 0 ppm, indicating aluminum in octahedral coordination. According to previous work [35], in which ^{27}Al MQ MAS NMR was used for studying the structure of beta zeolite with different Si/Al ratios, the positions of chemical shifts related to octahedral coordination depend on this ratio. For zeolites with low ratios, the shifts occur from 5 to -5 ppm and are related to aluminum, which can go back to tetrahedral position by heating or chemical treatment. These peaks are thus considered framework-associated octahedral aluminum. Therefore, the peaks at 5.7 ppm (B-H), 2.1 ppm (Ni3B-H) and -2.0 ppm (Ni5B-H) can be assigned to framework-associated octahedral aluminum. These species are produced by the partial hydrolysis of Si-O-Al bonds during calcination and largely depends on the pretreatment of beta zeolite, being related to Lewis acidity [38, 39]. Lewis acid sites (LAS) are formed due to the high electron affinity of a proton of a catalytic site [39]. It has been proposed [40] that the LAS activity is related to the ability of beta zeolite framework to create octahedral aluminum. Other broad peaks appeared in the spectra of nickel catalysts, as compared to B-H, at -12 ppm (Ni3B-H) and -16 ppm (Ni5B-H), which are related to extra-framework octahedral aluminum in asymmetric and heterogeneous environments, in accordance with previous works [35, 41, 42]. These peaks have been considered as an effect of calcination method [35, 42] or with cations in zeolite structure [41]. Both effects are believed to strongly affect the number and the type of octahedral aluminum species.

These results show that nickel increases the disorder of B-H, by changing the chemical environment of aluminum and then its chemical bonds in zeolite structure, which can result in different catalytic activities [43]. For all spectra, the peak related to tetrahedral aluminum was stronger than the peak associated to octahedral aluminum indicating that most of the aluminum atoms are in tetrahedral coordination in the framework. Table 2 shows that the relative amounts of tetrahedral aluminum increased due to the nickel presence, as can be seen in the aluminum in tetrahedral position to aluminum in octahedral position ratio ($\text{Al}_{\text{Td}}/\text{Al}_{\text{Oh}}$).

Regarding the ^{29}Si NMR spectra (Fig. 2b), several studies [38, 44, 45] have shown that beta zeolite has nine crystallographic non-equivalent tetrahedral (T) sites and then a complex spectrum is expected. However, only three signals are often detected even in high resolution spectra, instead of three groups of nine lines, due to the high concentration of stacking faults in beta zeolite structure. The silicon atoms at Q^3 and Q^2 sites Si(3Si,1OH) and Si(2Si,2OH) produced signals at -102 ppm and -94 ppm, respectively. These silicon atoms are bound to one or two defect groups. On the other hand, the signals at -111 ppm, -106 ppm and -98 ppm are related to silicon atoms at the Q^4 sites Si(4Si), Si(3Si,1Al) and Si(2Si,2Al). The ^{29}Si NMR spectra of beta zeolite shows a broad peak ranging from -80 to -120 ppm, centered at -104 ppm with a shoulder at -94 ppm, in agreement with other works [36, 44, 45]. According to previous assignments, this peak can be assigned to the superposition of signals, caused by silicon atoms at Q^2 , Q^3 and Q^4 sites. The signal at -104 ppm is the strongest one, suggesting the predominance of silicon atoms at the Si(3Si,1Al) and Si(3Si,1OH) sites. As stated previously [45], in samples with low Si/Al ratios, the signal at -104 ppm is related to the superposition of Si(3Si,1Al) at -106 ppm and Si(3Si,1OH) at -102 ppm.

The lines above -111 ppm would be expected in samples with high silicon content. This line seems to be weak in our sample. The nickel-containing samples displayed similar profiles, the Ni3B-H sample showing the peak with a maximum at -100 ppm. It indicates that the silicon crystallographic sites have slightly changed by nickel.

It is well-known [46] that beta zeolite has several suitable properties as catalyst including the large specific surface area and pore, high thermal stability and adjustable acidity, which largely depends on tetrahedral aluminum in zeolite framework. To better understand the acidic sites in the samples, results of NH_3 -TPD and FTIR of pyridine adsorption were used for catalysts characterization. Table 2 presents the distribution of acid sites (weak, strong, very strong and total) for the catalysts and the NH_3 -TPD profiles are shown in Fig. 3. We can see that B-H showed two peaks, in accordance with previous works [47, 48]. The first one, with a maximum desorption temperature between 145 and 163 °C (T1), is related to ammonia adsorbed on weak sites such as silanol groups. The second peak (T2), in the range of 337 to 363 °C, is related to ammonia molecules interacting with framework aluminum species and then are considered strong acid sites [49]. The introduction of nickel to B-H creates stronger acid sites (T3) and increased the amount of total acid sites, both effects increasing with nickel amount (Table 2).

The classification of acid sites (AS) of the samples in Brønsted (BAS) and Lewis (LAS) types has been performed using FTIR after adsorption of pyridine to B-H, Ni3B-H and Ni5B-H (Fig. 4). A first band (1545 cm^{-1}) is assigned to pyridine ion (protonation of pyridine in the BAS), whereas the other one (1445 cm^{-1}) refers to pyridine molecule interacting by coordination with the LAS. The band at 1490 cm^{-1} is related to the interaction of pyridine with both acidic sites (BAS and LAS) [50]. It can be noted that the BAS

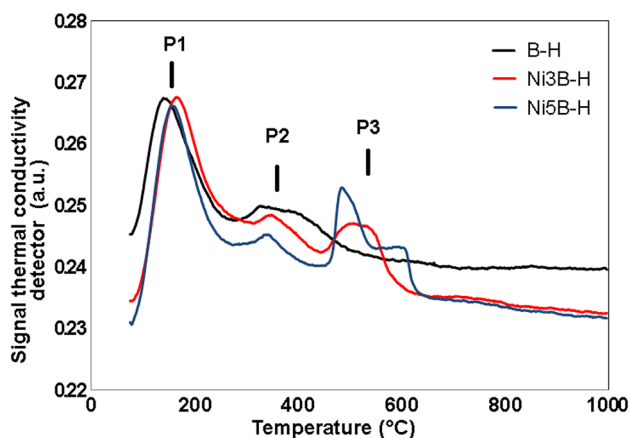


Fig. 3 NH_3 -TPD profile for B-H, Ni3B-H and Ni5B-H catalysts. P1: weak acid site; P2: strong acid site; P3: stronger acid site. "P" stands for "peak". Experimental procedures are described in Sects. Nickel-Modified Beta Zeolite Synthesis and Characterization

peaks were decreased by nickel, a fact that can be related to the replacement of some protons by nickel ions during impregnation. During this process, the proton of the BAS (Si-OH-Al) is substituted by the impregnated metal cation (Ni^{2+}), in accordance with a previous work [47]. In some cases, the reduction of BAS may be a consequence of the blocking of catalyst pores by the metal oxide [47]. However, we have not found a significant reduction in the pore volume of nickel catalysts which means that no significant blockage has occurred (Table 2).

The band at 1445 cm^{-1} (LAS) increased after nickel impregnation as compared with B-H. As concluded by NMR, after nickel addition, more aluminum atoms will occupy different crystallographic sites and more octahedral aluminum will be linked to beta framework, where they can change to tetrahedral positions [37]. As shown in Table 2, nickel increased the amount of aluminum in tetrahedral position in framework. In both positions, aluminum (octahedral and tetrahedral) can act as LAS [37]. However, it is known that extra-framework aluminum species are related to weak acid sites, whereas the framework aluminum species generate strong acid sites [51]. This explained the increase of weak sites caused by nickel, which increased the amount of extra-framework aluminum, evidenced by the peaks at -12 ppm (Ni3B-H sample) and -16 ppm (Ni5B-H) in ^{27}Al NMR spectra. On the other hand, the increased amount of strong sites caused by nickel can be explained by the higher amount of octahedral aluminum in the framework as shown by the peaks at 2.1 ppm (Ni3B-H) and -2.0 ppm (Ni5B-H) in ^{27}Al NMR spectra.

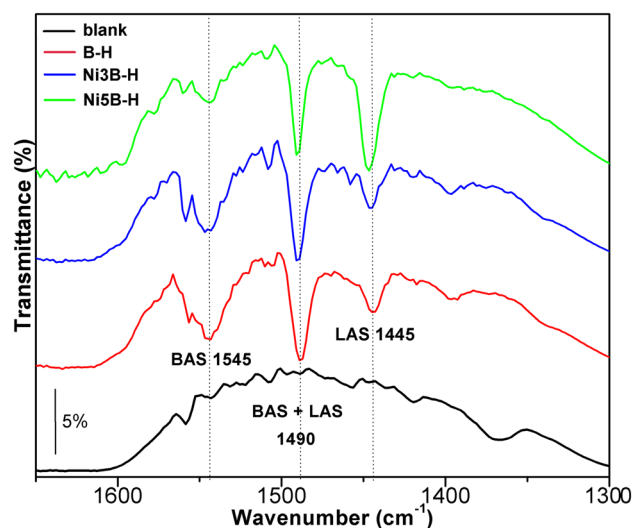


Fig. 4 Fourier transform infrared (FTIR) spectra obtained after pyridine adsorption on the catalysts. B-H: beta zeolite; Ni3B-H and Ni5B-H: beta zeolite with 3 and 5% of nickel, respectively. BAS Brønsted acid site, LAS Lewis acid site. Experimental procedures are described in Sects. Nickel-Modified Beta Zeolite Synthesis and Characterization

In addition, the increase of LAS and total amount acid sites (Table 2) are also related to nickel oxide which can act as a Lewis acid center. Iliopoulou et al. [52] have used HZSM-5 modified with different amounts (1, 5 e 10 wt/wt %) of nickel oxide and cobalt (II, III) oxide in the pyrolysis of a commercial lignocellulosic biomass (Lignocel HBS 150–500). They reported higher concentration of LAS after impregnation with nickel (43.9–54.9 $\mu\text{mol g}^{-1}$) and cobalt (35.4–45.9 $\mu\text{mol g}^{-1}$) when compared to HZSM-5 (18.1 $\mu\text{mol g}^{-1}$). The increase in LAS was attributed to the formation of the corresponding oxides of impregnated metals (NiO and Co_3O_4 , confirmed by XRD), which could act as Lewis' acid centers. Karakoulia et al. reported similar results for HZSM-5 zeolite with 10 wt% of nickel, prepared by wet impregnation [53].

Influence of Beta Zeolite on the Distribution of Aromatic Hydrocarbons in Pyrolysis Vapors

Table 3 shows the comparison between the compound classes tentatively identified in pyrolytic vapors. Non-catalytic pyrolysis produced mainly O-compounds (Table 3 and Online Resource 1 in Table ESM2). This distribution of products from pyrolytic vapors of pre-treated MDF residues in chemical classes is similar to the results found in a former study of our group, where non-treated MDF residues based on eucalyptus and pinus woods have been employed [10]. Other researchers have also found mainly phenolic compounds and other oxygenated classes, as for example, ketones in the bio-oil of wood-based panels [2]. No nitrogen compound has been identified in MDF pyrolysis vapors, as shown in Table 3 and Online Resource 1 in Table ESM2. It means that if small amounts of N-compounds remain in biomass after pre-treatment (Table 1), it will not be harmful

to people or environment, during pyrolysis process, neither to bio-oil quality.

The use of catalysts based on beta zeolite in the pyrolysis of pre-treated MDF residues drastically changed the composition of pyrolytic vapors (Table 3). The chromatographic area percentage of AH ranged from 70.20 to 85.40% for catalytic pyrolyses, while they were not detected in the non-catalytic bio-oil. The AH class was divided into MAH [composed of BTEX, OA (other aromatics: other alkyl benzenes, indane and its derivatives)] and PAH (naphthalenes and $\text{PAH} > 2$ rings, where $\text{PAH} > 2$ rings designate PAH whose structures contain more than two aromatic rings) (Table 3). In general, the higher the number of aromatic rings the more toxic is the PAH and this is the reason for classifying PAH according to two rings (naphthalenes) and more than two rings. MAH were the major class in the vapors of catalytic pyrolysis (48.69–61.61%). They were followed by PAH, which showed lower area (%) when modified catalysts were used in the process (11.12–36.71%). Oxygenated monoaromatic and polyaromatic hydrocarbons have not been found in vapor pyrolysis.

The chromatographic area (%) of O-compounds has been reduced from 76.01% (non-catalytic) to 0.67, 2.64 and 14.16% when B-H, Ni5B-H and Ni3B-H catalysts were employed, respectively. These can be related to the different selectivity of the catalysts towards each reaction during the catalytic pyrolyses of biomass. In fact, the activation energy of each reaction normally changes on different catalysts. Cracking, hydrodeoxygenation (HDO), oligomerization, cyclization, aromatization, alkylation, isomerization, polymerization, decarbonylation, decarboxylation, hydrocracking, hydrogenolysis, hydrogenation and others can take place on different kinds of catalytic sites, during catalytic pyrolysis of biomass, producing a complex network of reactions.

Table 3 General distribution of chromatographic area percentages of classes of compounds tentatively identified in the catalytic and non-catalytic pyrolysis vapors

| Compounds class | Aromatic hydrocarbons (AH) | | | | | | | |
|-----------------|---------------------------------|---------------|---------------|--------------------------------|------------------|---------------|---------------|---------------|
| | Monoaromatic hydrocarbons (MAH) | | | Polyaromatic hydrocarbon (PAH) | | | | |
| Catalytic | BTEX | OA | Σ MAH | Naphthalenes | $\text{PAH} > 2$ | Σ PAH | Σ AH | O-compounds |
| | Area% ^a /SD | | | | | | | |
| B-H | 23.51 ± 1.05b | 25.18 ± 0.27a | 48.69 ± 0.54a | 29.53 ± 1.10a | 7.18 ± 0.69b | 36.71 ± 1.26b | 85.40 ± 1.81a | 0.67 ± 0.01a |
| Ni3B-H | 39.35 ± 3.96a | 19.70 ± 3.66a | 59.08 ± 5.41a | 11.12 ± 0.79b | nd | 11.12 ± 0.79a | 70.20 ± 5.98a | 14.16 ± 4.47a |
| Ni5B-H | 38.65 ± 2.73a | 22.96 ± 3.47a | 61.61 ± 0.52a | 15.43 ± 0.36c | 0.49 ± 0.03a | 15.93 ± 0.36a | 77.54 ± 0.80a | 2.64 ± 0.42a |
| non-catalytic | nd | nd | nd | nd | nd | nd | nd | 76.01 ± 0.19b |

SD standard deviation, nd non detected; average values, in the same column, that are followed by the same letter (a, b, or c) are not significantly different from each other, according to Tukey's test ($p \leq 0.05$). Pure beta zeolite (B-H) and B-H modified with 3% (Ni3B-H) and 5% of nickel (Ni5B-H), BTEX benzene, toluene, ethylbenzene, xylenes, OA other aromatics, $\text{PAH} > 2$ polyaromatic hydrocarbons whose structure contain more than two aromatic rings; Experimental procedures are described in Sect. Catalytic and Non-Catalytic Analytical Pyrolysis

^aCalculated according to Sect. Catalytic and Non-Catalytic Analytical Pyrolysis

Among them, HDO is by far the most important one [54], being responsible for the production of water and for oxygen removal. Carboxylation is also a desirable reaction while decarbonylation is undesirable [47].

Among the catalysts, B-H performed especially well in oxygen removal of pyrolytic vapors of pre-treated MDF (99%) and also in the production of AH, which is an important achievement as it may provide higher bio-oil quality and stability. Similar results have been obtained in the catalytic pyrolyses of several biomasses (sunflower stem, cellulose, cedar, apple, and eucalyptus wood) over beta zeolite [47]. This is closely related to the inherent characteristics of beta zeolite such as high specific surface area, large pores and strong BAS and LAS. Because of the large pores of beta zeolite, the bulky molecules can enter in the channels, where they go on cracking, deoxygenation/hydrodeoxygenation, hydrogenation/dehydrogenation and other reactions on acidic sites. As shown by the results of NH_3 -TPD and FTIR, beta zeolite has strong Brönsted and Lewis acid sites generated by H^+ and Al^{3+} species. As pointed out earlier [54] these sites are able to catalyze cracking/hydrocracking, deoxygenation/HDO, hydrogenation/dehydrogenation and isomerization giving rise to aromatics and decreasing the amount of O-compounds.

Despite the excellent results obtained on B-H, the high levels of PAH produced over this catalyst deserve attention. PAH are highly toxic compounds and then are not desirable in transport fuels [19]. Indeed, it has been reported that beta zeolite produced higher content of PAH, when compared to other zeolites, such as HZSM-5 and H-modernite [18]. This fact is related to the larger pores of beta zeolite, which facilitate the diffusion of primary pyrolysis compounds and the production of PAH on the acid sites of the catalyst. However, this can increase coke production, resulting in deactivation of the catalyst [12, 16]. The high catalyst/biomass ratio (5/1) that ensured available acid sites for the reactants probably helped PAH formation, with eventual production of coke. The use of high catalyst/biomass ratios is common in pyrolysis and aims to ensure the access of all reactant to the active sites, especially in the cases where part of the catalysis can be deactivated by coke [16].

The introduction of nickel in beta zeolite provided the decrease of PAH. Their chromatographic area percentages changed from 36.71% (B-H) to 11.12% (Ni3B-H) and 15.93% (Ni5B-H). The chromatographic area percentage of naphthalene was significantly smaller for Ni3B-H (11.12%) than for Ni5B-H (15.43%), while PAH > 2 rings were not tentatively identified for Ni3B-H and reached a total of 0.49% of the chromatographic area percentage of vapors from catalytic pyrolysis over Ni5B-H (Table 3).

The use of nickel impregnated beta zeolites largely improved the selectivity of the catalysts towards BTEX (> 38%) in comparison with the use of B-H (23.51%). All

compounds of the BTEX mixture showed chromatographic areas significantly enhanced by nickel, as displayed in Fig. 5. The contribution of toluene was especially noted (B-H: 9.58%, Ni3B-H: 16.99% and Ni5B-H: 17.09%), followed by xylenes (B-H: 9.95%, Ni3B-H: 14.82% and Ni5B-H: 15.28%), benzene (B-H: 3.02%, Ni3B-H: 6.03% and Ni5B-H: 4.78%) and ethylbenzene (B-H: 0.77%, Ni3B-H: 1.46% and Ni5B-H: 1.48%). It is known that the BTEX mixture arouses interest in industry as precursor of many compounds. Toluene, for example, is used as raw material for the production of benzene and its derivatives and of drugs and dyes, among others. Moreover, *p*-xylene is used in the production of terephthalic acid, a precursor to polyethylene terephthalate (PET) which, in turn, is used in several other branches of industry [17, 24].

The efficiency of the nickel catalysts can be related to the changes in aluminum chemical environments related to crystallographic sites, changing the catalytic activity and the amount and strength of acid sites of the catalysts (Sect. [Catalyst Characterization](#)). The enhanced production of BTEX with nickel catalysts can be related to an increase of the activity of the catalysts in cracking/hydrocracking, hydrogenation/dehydrogenation and isomerization giving rise to aromatics, on the stronger sites of these catalysts. However, the amount of O-compounds increased, indicating lower activity of these catalysts in the reactions related to oxygen removal, mainly the HDO and deoxygenation. This finding suggests that the BAS are more active than LAS in HDO, in accordance with previous work [55]. Therefore, B-H is able to produce less

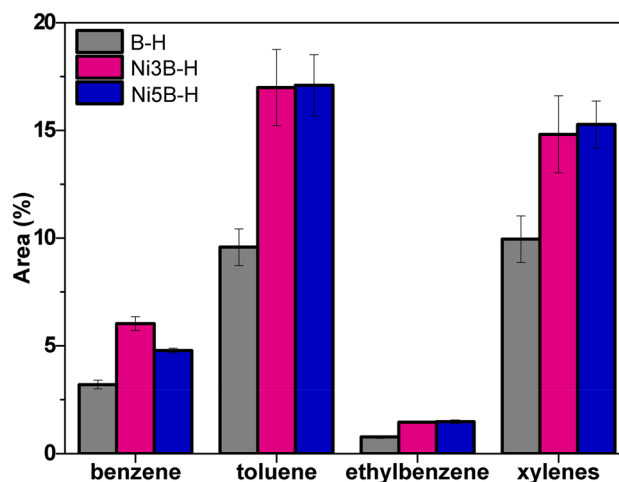


Fig. 5 Selectivity of the beta zeolite catalysts towards BTEX (benzene, toluene, ethylbenzene and xylenes) compounds contained in bio-oils produced by catalytic pyrolyses of pre-treated MDF residues. Ni3B-H and Ni5B-H are 3 and 5% nickel modified beta zeolite and B-H is a pure beta zeolite. Area (%): calculated according to Sect. [Catalytic and Non-Catalytic Analytical Pyrolysis](#). Experimental procedures are described in Sect. [Catalytic and Non-Catalytic Analytical Pyrolysis](#)

oxygenated products, as compared to nickel-containing catalysts, due to the stronger ability of H^+ species to react with oxygen atoms, as compared to LAS.

For the Ni5B-H sample, the amount of O-compounds was lower than for Ni3B-H, a fact that can be assigned to its higher number of stronger active sites, as shown in Table 2. In addition, nickel catalysts largely decreased the amount of naphthalenes and PAH > 2 rings, showing ability to open multi aromatic rings. This suggests that nickel itself plays a role in catalyzing some reactions during fast pyrolysis, besides changing the acidity of the solids. In a previous work, it has been demonstrated [52] that nickel can be reduced during fast pyrolysis of biomass, by hydrogen produced by cracking reactions, allowing the formation of metallic nickel and then of a bifunctional catalyst. These catalysts are characterized by the presence of acidic sites (originated from the support) and by metallic sites (reduced nickel). It is well known that bifunctional catalysts of nickel supported on beta zeolite are efficient in multi ring opening reactions with the aim of decreasing the PAH content in samples such as diesel and bio-residual tire oil due to nickel ability to break C–C bonds [17, 20]. The transformation of PAH, such as naphthalenes and its derivatives in MAH occurs in two stages. The first stage is associated with hydrogenation reactions of the aromatic rings on metal sites, forming tetralin or its derivatives. The second stage occurs on acidic sites, responsible for cracking the naphthenic ring, giving rise to compounds with only one aromatic ring (MAH, such as BTEX) [17, 21]. In our work, it was not possible to identify metallic nickel in the spent catalysts, since the pyrolysis experiments were performed on analytical scale.

These results show that the drawback related to beta zeolite concerning the production of toxic PAH can be largely overcome by introducing nickel on the zeolite by impregnation. In addition, the activity of the catalysts for different reactions can be tailored for different purposes. Among the catalysts, Ni5B-H is the most efficient catalyst to produce a bio-oil rich in BTEX and with no content of highly toxic compounds, such as PAH and low content of O-compounds.

Conclusion

A simple process of washing MDF with hot water at 80 °C efficiently removed N-compounds from MDF residues. This strongly suggests that this method can be advantageously applied in pilot or industrial plants before the pyrolysis of MDF residues. The nickel-containing catalysts have been proved to be promising for the production of bio-oil rich in BTEX and with low content of O-compounds or no content of toxic PAH, depending on the application. These results showed interesting perspectives for the use of MDF residues and an improvement related to the production of a bio-oil with higher concentrations of BTEX.

Supplementary Information The online version contains supplementary material available at <https://doi.org/10.1007/s12649-021-01593-w>.

Acknowledgements The authors thank the National Council for Scientific and Technological Development (CNPq, *Conselho Nacional de Desenvolvimento Científico e Tecnológico*) and the Brazilian Federal Agency for Support and Evaluation of Graduate Education (CAPES, *Coordenação de Aperfeiçoamento de Pessoal de Nível Superior*), for financial support through research projects and scholarships (F. Mayer's DSc CAPES 1511161 and C. Zini's researcher scholarship CNPq 306067/2016-1). The authors thank Renato Bernardi from SENAI for helping with MDF sampling and milling.

Funding Partial financial support was received from National Council for Scientific and Technological Development (CNPq, *Conselho Nacional de Desenvolvimento Científico e Tecnológico*) and the Brazilian Federal Agency for Support and Evaluation of Graduate Education (CAPES, *Coordenação de Aperfeiçoamento de Pessoal de Nível Superior*), through research projects and scholarships (F. Mayer's DSc CAPES 1511161 and C. Zini's researcher scholarship CNPq 306067/2016-1).

Data Availability All data generated or analyzed during this study are included in this published article [and its supplementary information files].

Declarations

Conflict of interests The authors have no conflicts of interest to declare that are relevant to the content of this article.

References


1. IBÁ - Indústria Brasileira de Árvores, 2020. Anual report. <https://www.iba.org/publicacoes/relatorios>. Accessed Dec 2020
2. Mu, J., Lai, Z.: Pyrolysis characteristics of wood-based panels and its products. In: Pyrolysis, pp. 52–70 (2017). <https://doi.org/10.5772/67506>
3. Hassan, S.S., Williams, G.A., Jaiswal, A.K.: Emerging technologies for the pretreatment of lignocellulosic biomass. *Bioresour. Technol.* (2018). <https://doi.org/10.1016/j.biortech.2018.04.099>
4. Zabed, H.M., Akter, S., Yun, J., Zhang, G., Awad, F.N., Qi, X., Sahu, J.N.: Recent advances in biological pretreatment of microalgae and lignocellulosic biomass for biofuel production. *Renew. Sustain. Energy Rev.* (2019). <https://doi.org/10.1016/j.rser.2019.01.048>
5. Miao, L., Yang, G., Tao, T., Peng, Y.: Recent advances in nitrogen removal from landfill leachate using biological treatments: a review. *J. Environ. Manage.* (2019). <https://doi.org/10.1016/j.jenvman.2019.01.057>
6. Toyama, T., Hanaoka, T., Tanaka, Y., Morikawa, M., Mori, K.: Comprehensive evaluation of nitrogen removal rate and biomass, ethanol, and methane production yields by combination of four major duckweeds and three types of wastewater effluent. *Bioresour. Technol.* (2018). <https://doi.org/10.1016/j.biortech.2017.11.054>
7. Grigsby, W.J., Carpenter, J.E.P., Sargent, R.: Investigating the extent of urea formaldehyde resin cure in medium density fiberboard: resin extractability and fiber effects. *J. Wood Chem. Technol.* (2014). <https://doi.org/10.1080/02773813.2013.861850>

8. Chen, D., Mei, J., Li, H., Li, Y., Lu, M., Ma, T., Ma, Z.: Combined pretreatment with torrefaction and washing using torrefaction liquid products to yield upgraded biomass and pyrolysis products. *Bioresour. Technol.* (2017). <https://doi.org/10.1016/j.biortech.2016.12.088>
9. Chen, D., Cen, K., Jing, X., Gao, J., Li, C., Ma, Z.: An approach for upgrading biomass and pyrolysis product quality using a combination of aqueous phase bio-oil washing and torrefaction pretreatment. *Bioresour. Technol.* (2017). <https://doi.org/10.1016/j.biortech.2017.02.120>
10. Mayer, F.M., Teixeira, C.M., Pacheco, J.G.A., Souza, C.T., Bauer, D.V., Caramão, E.B., Espíndola, J.S., Trierweiler, J.O., Perez-Lopez, O.W., Zini, C.A.: Characterization of analytical fast pyrolysis vapors of medium-density fiberboard (MDF) using metal-modified HZSM-5. *J. Anal. Appl. Pyrolysis* (2018). <https://doi.org/10.1016/j.jaap.2018.10.019>
11. Kabir, G., Hameed, B.H.: Recent progress on catalytic pyrolysis of lignocellulosic biomass to high-grade bio-oil and bio-chemicals. *Renew. Sustain. Energy Rev.* (2017). <https://doi.org/10.1016/j.rser.2016.12.001>
12. Rahman, M.M., Liu, R., Cai, J.: Catalytic fast pyrolysis of biomass over zeolites for high quality bio-oil: a review. *Fuel Process. Technol.* (2018). <https://doi.org/10.1016/j.fuproc.2018.08.002>
13. Huang, M., Ma, Z., Zhou, B., Yang, Y., Chen, D.: Enhancement of the production of bio-aromatics from renewable lignin by combined approach of torrefaction deoxygenation pretreatment and shape selective catalytic fast pyrolysis using metal modified zeolites. *Bioresour. Technol.* (2020). <https://doi.org/10.1016/j.biortech.2020.122754>
14. Huang, M., Xu, J., Ma, Z., Yang, Y., Zhou, B., Wu, C.: Bio-BTX production from the shape selective catalytic fast pyrolysis of lignin using different zeolite catalysts: relevance between the chemical structure and the yield of bio-BTX. *Fuel Process. Technol.* (2021). <https://doi.org/10.1016/j.fuproc.2021.106792>
15. Liu, R., Sarker, M., Rahman, M., Li, C., Chai, M., Cotillon, R., Scott, N.R.: Multi-scale complexities of solid acid catalysts in the catalytic fast pyrolysis of biomass for bio-oil production: a review. *Prog. Energy Combust. Sci.* (2020). <https://doi.org/10.1016/j.pecs.2020.100852>
16. Mihalcik, D.J., Mullen, C.A., Boateng, A.A.: Screening acidic zeolites for catalytic fast pyrolysis of biomass and its components. *J. Anal. Appl. Pyrolysis* (2011). <https://doi.org/10.1016/j.jaap.2011.06.0011>
17. Namchot, W., Jitkarnka, S.: Impacts of nickel supported on different zeolites on waste tire derived oil and formation of some petrochemicals. *J. Anal. Appl. Pyrolysis* (2016). <https://doi.org/10.1016/j.jaap.2016.01.001>
18. Yu, Y., Li, X., Su, L., Zhang, Y., Wang, Y., Zhang, H.: The role of shape selectivity in catalytic fast pyrolysis of lignin with zeolite catalysts. *Appl. Catal. A Gen.* (2012). <https://doi.org/10.1016/j.apcata.2012.09.012>
19. Varjani, S.J., Gnansounou, E., Pandey, A.: Comprehensive review on toxicity of persistent organic pollutants from petroleum refinery waste and their degradation by microorganisms. *Chemosphere* (2017). <https://doi.org/10.1016/j.chemosphere.2017.09.005>
20. Lee, S., Lee, Y., Kim, J., Jeong, S.: Tactical control of Ni-loading over W-supported beta zeolite catalyst for selective ring opening of 1-methylnaphthalene. *J. Ind. Eng. Chem.* (2018). <https://doi.org/10.1016/j.jiec.2018.05.042>
21. Choi, Y., Lee, J., Shin, J., Lee, S., Kim, D., Lee, J.K.: Selective hydroconversion of naphthalenes into light alkyl-aromatic hydrocarbons. *Appl. Catal. A Gen.* (2015). <https://doi.org/10.1016/j.apcata.2014.12.001>
22. Escola, J.M., Aguado, J., Serrano, D.P., Briones, L., Díaz De Tuesta, J.L., Calvo, R., Fernandez, E.: Conversion of polyethylene into transportation fuels by the combination of thermal cracking and catalytic hydroreforming over Ni-supported hierarchical beta zeolite. *Energy Fuels* (2012). <https://doi.org/10.1021/ef300938r>
23. Fonseca, J.S.L., Júnior, A.C.F., Grau, J.M., Rangel, M.C.: Ethylbenzene production over platinum catalysts supported on modified KY zeolites. *Appl. Catal. A Gen.* (2010). <https://doi.org/10.1016/j.apcata.2010.07.056>
24. Galadima, A., Muraza, O.: In situ fast pyrolysis of biomass with zeolite catalysts for bioaromatics/gasoline production: a review. *Energy Convers. Manag.* (2015). <https://doi.org/10.1016/j.enconman.2015.07.078>
25. van Rij, N.J.W.K.: The yeasts a taxonomic study. In: Elsevier (ed.), third edit, Amsterdam, p. 1082 (1984)
26. Yarrow, D.: Methods for the isolation, maintenance and identification of yeasts. In: C.P.K. and J.W. Fell (eds.), pp. 77–100 (1998)
27. Vaudry, F., Di Renzo, F., Espiau, P., Fajula, F.: Aluminum-rich zeolite beta. *Zeolites* **19**, 253 (1997). [https://doi.org/10.1016/S0144-2449\(97\)00083-3](https://doi.org/10.1016/S0144-2449(97)00083-3)
28. Bhat, R.N., Kumar, R.: Synthesis of zeolite beta using silica gel as a source of SiO₂. *J. Chem. Technol. Biotechnol.* **48**, 453 (1990). <https://doi.org/10.1002/jctb.280480407>
29. Nuffield, E.W.: X-Ray Diffraction Methods. EUA, New York (1986)
30. Dhyani, V., Bhaskar, T.: A comprehensive review on the pyrolysis of lignocellulosic biomass. *Renew. Energy.* (2018). <https://doi.org/10.1016/j.renene.2017.04.035>
31. Pereira, A.L.C., González-Carbalho, J.M., Pérez-Afonso, F.J., Rojas, S., Fierro, J.L.G., Rangel, M.C.: Effect of the mesostructure of the beta zeolite support on the properties of cobalt catalysts for Fischer–Tropsch synthesis. *Top Catal.* (2011). <https://doi.org/10.1007/s11244-011-9637-6>
32. Grecco, S.T.F., Rangel, M.C.: Hierarchically structured zeolites. *Quim. Nova* (2013). <https://doi.org/10.1590/S0100-40422013000100023>
33. Dirken, P.J., Kentgens, A.P.M., Nachtegaal, G.H., Van Der Eerden, A.M.J., Jansen, J.B.H.: Solid-state MAS NMR study of pentameric aluminosilicate groups with 1800 intertetrahedral Al–Q–Si angles in zunyite and harkerite. *Am. Miner.* **80**, 39–45 (1995)
34. Kadgaonkar, M.D., Kasture, M.W., Bhange, D.S., Joshi, P.N., Ramaswamy, V., Kumar, R.: NCL-7, a novel all silica analog of polymorph B rich member of BEA family: synthesis and characterization. *Microporous Mesoporous Mater.* (2007). <https://doi.org/10.1016/j.micromeso.2006.10.033>
35. Abraham, A., Lee, S., Shin, C., Hong, S.B., Prins, R., Van Bokhoven, J.A.: Influence of framework silicon to aluminium ratio on aluminium coordination and distribution in zeolite beta investigated by ²⁷Al MAS and ²⁷Al MQ MAS NMR. *Phys. Chem. Chem. Phys.* (2004). <https://doi.org/10.1039/B401235F>
36. Zaykovskaya, A.O., Kumar, N., Kholkina, E.A., Li-zhulanov, N.S., Aho, A., Peltonen, J., Peurla, M., Heinmaa, I., Yu, D.: Synthesis and physico-chemical characterization of Beta zeolite catalysts: evaluation of catalytic properties in Prins cyclization of (–)-isopulegol. *Microporous Mesoporous Mater.* (2020). <https://doi.org/10.1016/j.micromeso.2020.110236>
37. Kunkeler, P.J., Zuurdeeg, B.J., Van Der Waal, J.C., Van Bokhoven, J.A.: Zeolite beta: the relationship between calcination procedure, aluminum configuration, and Lewis acidity. *J. Catal.* (1998). <https://doi.org/10.1006/jcat.1998.2273>
38. Wouters, B.H., Chen, T., Grobet, P.J.: Reversible Tetrahedral - Octahedral framework aluminum transformation in zeolite Y. *J. Am. Chem. Soc.* (1998). <https://doi.org/10.1021/ja9820821>
39. Bourgeat-lami, E., Massiani, P., Di Renzo, F., Espiau, P., Fajula, F.: Study of the state of aluminium in zeolite-beta. *Appl. Catal.* (1991). [https://doi.org/10.1016/0166-9834\(91\)85034-S](https://doi.org/10.1016/0166-9834(91)85034-S)
40. Van Bokhoven, J.A., Koningsberger, D.C., Kunkeler, P., Van Bekkum, H.: Influence of steam activation on pore structure and acidity of zeolite beta: an Al K Edge XANES study of aluminum

- coordination. *J. Catal.* (2002). <https://doi.org/10.1006/jcat.2002.3777>
41. Korányi, T.I., Nagy, J.B.: Distribution of aluminum in different periodical building units of MOR and BEA zeolites. *J. Phys. Chem. B* (2005). <https://doi.org/10.1021/jp051793k>
 42. Camblor, M.A., Corma, A., Valencia, S.: Synthesis in fluoride media and characterisation of aluminosilicate zeolite beta. *J. Mater. Chem.* (1998). <https://doi.org/10.1039/A804457K>
 43. Freude, H.-J.B.D.: Investigation of ^{27}Al -NMR chemical shifts in zeolites of the faujasite type. *Cryst. Res. Technol.* (1981). <https://doi.org/10.1002/crat.19810160322>
 44. Stelzer, J., Paulus, M., Hunger, M., Weitkamp, J.: Hydrophobic properties of all-silica zeolite beta. *Microporous Mesoporous Mater.* (1998). [https://doi.org/10.1016/S1387-1811\(98\)00071-7](https://doi.org/10.1016/S1387-1811(98)00071-7)
 45. Pérez-Pariente, J., Sanz, J., Fornés, V., Corma, A.: ^{29}Si and ^{27}Al MAS NMR study of zeolite beta with different Si/Al ratios. *J. Catal.* (1990). [https://doi.org/10.1016/0021-9517\(90\)90116-2](https://doi.org/10.1016/0021-9517(90)90116-2)
 46. Yue, Y., Guo, X., Liu, T., Liu, H., Wang, T., Yuan, P., Zhu, H., Bai, Z., Bao, X.: Template free synthesis of hierarchical porous zeolite beta with natural kaolin clay as alumina source. *Microporous Mesoporous Mater.* (2020). <https://doi.org/10.1016/j.micro-meso.2019.109772>
 47. Hernando, H., Moreno, I., Feroso, J., Ochoa-hernández, C., Pizarro, P., Coronado, J.M., Serrano, D.P.: Biomass catalytic fast pyrolysis over hierarchical ZSM-5 and beta zeolites modified with Mg and Zn oxides. *Biomass Convers. Biorefinery* (2017). <https://doi.org/10.1007/s13399-017-0266-6>
 48. Grecco, S.T.F., Urquieta-González, E.A., Reyes, P., Oportus, M., Rangel, M.C.: Influence of temperature and time of seed aging on the properties of beta zeolite/MCM-41 materials. *J. Braz. Chem. Soc.* (2014). <https://doi.org/10.5935/0103-5053.20140271>
 49. Serrano, D.P., Vicente, G., Linares, M.: Acidic and catalytic properties of hierarchical zeolites and hybrid ordered mesoporous materials assembled from MFI protozeolitic units. *J. Catal.* (2011). <https://doi.org/10.1016/j.jcat.2011.02.007>
 50. Benaliouche, F., Boucheffa, Y.: NH_3 -TPD and FTIR spectroscopy of pyridine adsorption studies for characterization of Ag- and Cu-exchanged X zeolites. *Microporous Mesoporous Mater.* (2008). <https://doi.org/10.1016/j.micromeso.2007.07.006>
 51. Srivastava, R., Iwasa, N., Fujita, S., Arai, M.: Dealumination of zeolite beta catalyst under controlled conditions for enhancing its activity in acylation and esterification. *Catal. Lett.* (2009). <https://doi.org/10.1007/s10562-009-9992-0>
 52. Iliopoulou, E.F., Stefanidis, S.D., Kalogiannis, K.G., Delimitis, A., Lappas, A.A., Triantafyllidis, K.S.: Catalytic upgrading of biomass pyrolysis vapors using transition metal-modified ZSM-5 zeolite. *Appl. Catal. B Environ.* **10**, 20 (2012). <https://doi.org/10.1016/j.apcatb.2012.08.030>
 53. Karakoulia, S.A., Heracleous, E., Lappas, A.A.: Mild hydroisomerization of heavy naphtha on mono- and bi-metallic Pt and Ni catalysts supported on beta zeolite. *Catal. Today.* (2020). <https://doi.org/10.1016/j.cattod.2019.04.072>
 54. Mortensen, P.M., Grunwaldt, J.D., Jensen, P.A., Knudsen, K.G., Jensen, A.D.: A review of catalytic upgrading of bio-oil to engine fuels. *Appl. Catal. A Gen.* (2011). <https://doi.org/10.1016/j.apcata.2011.08.046>
 55. Chen, H., Cheng, H., Zhou, F., Chen, K., Qiao, K., Lu, X., Ouyang, P.: Catalytic fast pyrolysis of rice straw to aromatic compounds over hierarchical HZSM-5 produced by alkali treatment and metal-modification. *J. Anal. Appl. Pyrolysis* (2018). <https://doi.org/10.1016/j.jaap.2018.02.009>

Publisher's Note Springer Nature remains neutral with regard to jurisdictional claims in published maps and institutional affiliations.

Authors and Affiliations

Francieli Martins Mayer^{1,2} · Ana Paula Stelzer de Oliveira¹ · Daliomar Lourenço de Oliveira Junior³ · Bruna Carla Agustini⁴ · Gildo Almeida da Silva⁴ · Eduardo Hiromitsu Tanabe³ · Doris Ruiz⁵ · Maria do Carmo Rangel^{1,2} · Claudia Alcaraz Zini¹ 

¹ Instituto de Química, Graduate Program in Chemistry, PPGQ, Universidade Federal do Rio Grande do Sul, UFRGS, Av. Bento Gonçalves, 9500, Porto Alegre, RS 91501-970, Brazil

² Instituto Nacional de Ciência, Tecnologia e Inovação em Materiais Complexos Funcionais (Inomat), Campinas, São Paulo, Brazil

³ Departamento de Engenharia Química, Universidade Federal de Santa Maria, UFSM, Santa Maria, RS, Brazil

⁴ Brazilian Agricultural Research Corporation (EMBRAPA) Grape & Wine, Bento Gonçalves, RS, Brazil

⁵ Facultad de Ciencias Químicas, Universidad de Concepción, Casilla 160-C, Concepción, Chile